A Modeling of Pump Impeller Shroud and Wear-Ring Seal as a Whole, and Its Application to the Pump Rotordynamics

Tae Woong Ha* and An Sung Lee**

(*Received July 15, 1997*)

A modeling methodology of pump impeller shroud and wear-ring seal as a whole has been developed to give its rotordynamic coefficients. In this work the governing equations are derived for the continuous flow path of the impeller shroud and wear-ring seal. Pressure loss at the discontinuity of the connecting point between the impeller shroud and the wear-ring seal is defined by utilizing a pressure loss coefficient obtained from experimental measurements. The governing equations are solved directly by using the known conditions at the inlet of the impeller shroud and the outlet of the wear-ring seal. A detailed rotordynamic analysis has been carried out on a 750 m-head fourteen-stage centrifugal pump system with the effects of the hydrodynamic forces of such as impeller shroud and wear-ring seals, balance piston, and interstage seals. Results have shown that the first critical speed obtained with all the seal effects is much higher than that obtained without those effects, and moreover that the system under consideration is unstable. Large cross coupled stiffness (k) of the impeller shroud and wear-ring seal has been suspected as the source of the problem. Design modifications of the impeller shroud and wear-ring seal geometry have been performed to decrease k and increase the direct damping (C). Finally, the design modifications have yielded a stable and well damped system.

Key Words: Rotordynamic Analysis, Centrifugal Pump, Impeller Shroud, Wear-Ring Seal, Critical Speed, Mode Shape.

Nomenclature

C, c : Direct and cross-coupled damping coefficients (N · s/m)
C_i : Inlet clearance of impeller shroud (mm)
C_p : Pressure loss coefficient in Eq. (8)
f : Frequency ratio in Eq. (10)
f_s, f_r : Fanning friction factor of stator and rotor surface in Eq. (4)
F_W, F_Y : Components of seal reaction force in X-Y coordinate system (N)
F_r, F_θ : Components of seal reaction force in R -θ coordinate system (N)
H : Local clearance (mm)
K, k : Direct and cross-coupled stiffness (N/m)
Ls : Impeller shroud surface length in path coordinate (m)
P : Pressure (bar)
R : Local radius (m)
R_i : Inlet radius of impeller shroud (m)
S : Path coordinate
s : Nondimensionalized path coordinate
t : time (s)
U_s, U_r : Bulk-flow velocities relative to stator and rotor of Eq. (4)
W_s, U_θ : Fluid velocity in the path and circumferential direction (m/s)
V : Fluid velocity (m/s)
V_i : Fluid velocity at impeller shroud entrance (m/s)
X, Y : Rotor displacements from its static position (m)
Z : Axial coordinate

* Assistant professor Architectural Equipment Engineering Department Kyung-won University Sungnam, Korea
** Senior Researcher, Rotor Dynamics Group Korea Institute of Machinery and Materials Daejeon, 305-600, Republic of Korea

ε : Eccentricity ratio
ρ : Fluid density (kg/m^3)
ξ : Inlet loss coefficient in Eq. (7)
γ : Slope of impeller shroud in Fig. 2
ω : Rotor angular velocity (rad/s)

Subscripts

a : Reservoir
0, 1 : Zeroth and first-order perturbations

1. Introduction

In multi-stage centrifugal pumps the hydrodynamic forces exerted by fluid-filled gaps such as impeller shroud and wear-ring seals, balance pistons, and interstage seals have tremendous influence on the rotordynamic behavior of the pumps, namely, critical speeds, stabilities, and imbalance response characteristics (Childs, 1993, Wachel et al., 1995). Therefore, their rotordynamic coefficients need to be accurately estimated so that analysis models should represent their real systems as closely as possible. There have been many works reported concerning critical speed analyses of multi-stage centrifugal pumps and the effects of the seals on the pump criticals (Atkins et al., 1985, Bowman et al., 1990, Frei et al., 1990). But none of these works have considered the effects of impeller shroud. In such conventional modeling practices the shrouds effects are often ignored by simply arguing that the shroud clearances are usually of one order higher than the wear-ring seal clearances but without further detailed justifications.

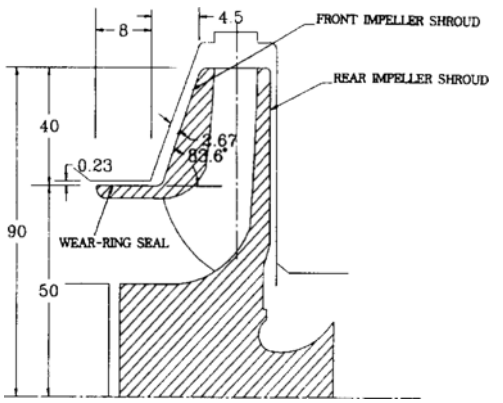

Fig. 1 Typical stage of a fourteen-stage centrifugal pump (unit : mm)

Figure 1 illustrates an impeller geometry of a fourteen-stage centrifugal pump, whose head and flowrate are 750 m and 30 m^3/h. As shown in Fig. 1, leakage along the front impeller shroud, from the impeller discharge to the inlet, is restricted by the wear-ring seal, while leakage along the rear impeller shroud is restricted by either an interstage seal or a balance piston. The lateral hydrodynamic force is developed along the front impeller shroud and wear-ring seal.

Several efforts have been made to theoretically predict the rotordynamic characteristics of pump annular seals, whose results are applicable to the analysis of balance pistons, interstage seals, and wear-ring seals (Black et al., 1970, Childs, 1983, Childs et al., 1985, Nordmann et al., 1984). However, a theoretical analysis for predicting rotordynamic coefficients of the front impeller shroud has been only performed by Childs (1989). Childs has extended his previous techniques in annular seal analysis and applied them to the flow within the clearance space between the housing and impeller shroud surface, which has some amount of slope against the axial direction.

In this work, modeling of the impeller shroud and wear-ring seal as a whole is suggested because of concerning their continuous passage. The current mathematical model follows basically Childs's derivation of the governing equations. However, the solution procedure is different. Their rotordynamic characteristices are thoroughly investigated as functions of the operating conditions and geometry variations. These results along with other seal effects are applied to a rotordynamic analysis of a fourteen-stage centrifugal pump system. The rotordynamic analysis is based on a finite element model (Ruhl and Booker, 1972, Zorzi and Nelson, 1977, Lalanne and Ferraris, 1990). Dry (ignoring any seal effects) and wet (involving seal effects) analyses are performed to investigate the effects of impeller shrouds and seals on the pump rotordynamics.

2. Rotordynamic Analysis of Impeller Shroud and Wear-Ring Seal as a Whole

As shown in Fig. 1, the impeller shroud and wear-ring seal forms one flow passage with discontinuity, where large clearance and flow direction change occur at the connecting point between the impeller shroud and the wear-ring seal. The geometrical difference between the impeller shroud annulus and the wear-ring seal annulus is that the impeller shroud's surface has some amount of slope against the rotor axis, while the wear-ring seal's surface has zero slope. Therefore, the governing equations of the impeller shroud annulus can be used for that of the wear-ring seal annulus setting the slope to zero. In the present work, the governing equations are derived for the continuous flow path of the impeller shroud and wear-ring seal. Additional pressure loss at the discontinuity of the connecting point between the impeller shroud and the wear-ring seal is defined by using a pressure loss coefficient determined from experimental measurements. The governing equations are solved directly by using the known conditions at the inlet of the impeller shroud and the outlet of the wear-ring seal while Childs analyzed separately the impeller shroud part and the wear-ring seal part and finally added them to calculate the rotordynamic coefficients of the impeller shroud and wear-ring seal.

2.1 Governing equations for impeller shroud annulus

Figure 2 shows the simplified impeller shroud geometry of Fig. 1 and a coordinate system for theoretical analysis. Based on Hirs(1973)' bulk-flow approach and Blasius' surface friction factor model, three equations for continuity, path-momentum, and circumferential momentum are derived for the impeller shroud annulus as shown in Eqs. (1) ~ (3).

Continuity :

$$\frac{\partial H}{\partial t}+\frac{\partial}{\partial S}(W_S H)+\frac{1}{R}\frac{\partial}{\partial \theta}(U_\theta H)+\frac{H}{R}\frac{\partial R}{\partial S} W_S=0 \tag{1}$$

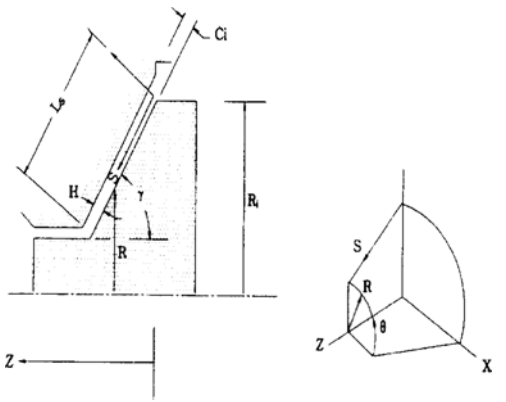

Fig. 2 Configuration of impeller shroud and wear-ring seal and coordinate system.

Path-momentum :

$$-H\frac{\partial P}{\partial S}=\frac{\rho}{2}f_s W_S U_s+\frac{\rho}{2}f_r W_S U_r+\rho H\left\{\frac{\partial}{\partial}t(W_S)\frac{\partial}{\partial S}(W_S)+\frac{U_\theta}{R}\frac{\partial}{\partial\theta}(W_S)\right\}-\rho H\frac{U_\theta^2}{R}\frac{dR}{dS} \tag{2}$$

Circumferential momentum :

$$-\frac{H}{R}\frac{\partial P}{\partial\theta}=\frac{\rho}{2}U_\theta U_s f_s+\frac{\rho}{2}(U_\theta-R\omega)U_r f_r+\rho H\left\{\frac{\partial}{\partial t}(U_\theta)+\frac{U_\theta}{R}\frac{\partial U_\theta}{\partial\theta}+W_S\frac{\partial U_\theta}{\partial S}+\frac{U_\theta W_S}{R}\frac{dR}{dS}\right\} \tag{3}$$

where

$$U_s=(W_S^2+U_\theta^2)^{\frac{1}{2}}$$
$$U_r=(W_S^2+(U_\theta-R\omega)^2)^{\frac{1}{2}}$$
$$f_s=ns\left(\frac{2\rho H U_s}{\mu}\right)^{ms} \tag{4}$$
$$f_r=nr\left(\frac{2\rho H U_r}{\mu}\right)^{mr}$$

The last terms of the path-momentum and circumferential momentum equation describe the centrifugal and the Coriolis acceleration of the fluid element, respectively. These terms will disappear for the wear-ring seal problem because the slope is zero(dR/dS=0). vm_s and f_r are the stator and rotor surface friction factors defined by the Blasius model. (ns, ms) and (nr, mr) are empirical coefficients depending on surface roughness of the stator(housing) and rotor (impeller shroud), respectively. The clearance (H) between the impeller shroud and housing can

be defined as Eq. (5) for small whirling motions of the impeller.

$$H(S, \theta, t) = H_0(S) - X\cos\gamma\cos\theta - Y\cos\gamma\sin\theta \quad (5)$$

2.2 Solution procedure

For the rotordynamic analysis of continuous annulus paths from the inlet of the impeller shroud to the exit of the wear-ring seal as a whole, the governing equations may be derived by combining the set of governing equations for the impeller shroud part(Eqs. (1)$\sim$(3)) and the wear-ring seal part. As previously mentioned, the governing equations for the wear-ring seal part corresponds to the case of dR/dS=0 of Eqs. (1)$\sim$(3). Assuming small whirling motion of the rotor about its geometric center, the path velocity, circumferential velocity, pressure, and local clearance can be expanded in terms of zeroth-order and first-order nondimensionalized perturbation variables:

$$w_s = w_{s0} + \varepsilon w_{s1}, \quad u_\theta = u_{\theta 0} + \varepsilon u_{\theta 1}$$
$$p = p_0 + \varepsilon p_1, \quad h = h_0 + \varepsilon h_1 \quad (6)$$
$$E = \frac{e}{C_i}$$

Substitution of these perturbed variables into the governing equations yields sets of zeroth-order and first-order equations. The nonlinear zeroth-order equations are numerically integrated using a Runge-Kutta method to yield matched boundary conditions. Known boundary values of pressure and circumferential velocity at the impeller shroud inlet and pressure at the wear-ring seal exit are served. The inlet pressure boundary condition at the impeller shroud entrance ($S=0$) is defined in terms of the inlet loss coeffcient(ζ) which depends on the entrance geometry:

$$p_0(0) = \frac{P_a}{\rho V_i^2} - (1-\zeta)\frac{w_{s0}(0)^2}{2} \quad (7)$$

Further, additional head loss of the discontinuity may occur at the connecting point between the impeller shroud and the wear-ring seal. For simplicity, pressure loss at the discontinuity can be defined in a manner similar to the loss of abrupt contration in pipe flow(Massey, 1986).

$$\Delta p = C_p\frac{\rho}{2}V^2 \quad (8)$$

The pressure loss coefficient C_p is closely related to the ratio of cross-sectional area. For coaxial circular pipes and fairly high Reynolds number flow, the value of C_p converges to 0.5 as the ratio of cross sectional area(A_2/A_1) approaches to zero. Though the ratio of cross sectional area at the interface of the impeller shroud and wear-ring seal approacher to zero($A_2/A_1=0.08$), the flow for the impeller shroud and wear-ring seal annulus might not be similar to the flow for the coaxial circular pipe. Therefore, experimental measurements are needed to determine C_p. Pressures are measured at three points, i. e., at the inlet of the impeller shroud, at the connecting point between the impeller shroud and wear-ring seal, and at the exit of the wear-ring seal for one impeller stage using a Bourdon pressure gauge whose resolution is 0.1% of the maximum pressure range. Figure 3 shows the comparison between the theoretical pressure result of the zeroth-order solution and three points of experimental measurements. In our theoretical analysis, 0.1 is used for the inlet loss coefficient ζ. As shown in Fig. 3, the pressure drops gradually through the impeller shroud leakage path% and drops very steeply at the interface of the impeller shroud and wear-ring seal($S=0.84$), and then drops sharply through the wear-ring seal leakage path to meet the exit pressure of the wear-ring seal. As the clearance of the impeller shroud is much bigger than that of

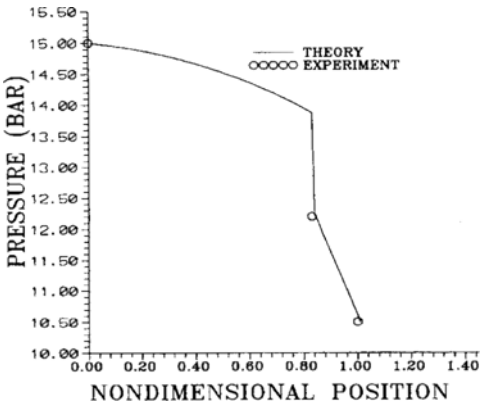

Fig. 3 Pressure distribution through the impeller shroud and wear-ring seal.

the wear-ring seal, the pressure drop of the seal part shows a sharper slope than that of the shroud part. Big pressure drop yields at the interface of the shroud and wear-ring seal due to the abrupt cross sectional contraction ($A_2/A_1=0.08$) and the change of flow direction. C_p is iteratively changed in the zeroth-order solution until the theoretical pressure at the interface meets the experimental measurement. Finally, 0. 6 is determined to be the value of C_p.

Along with the results of the zeroth-order solution, the first-order perturbation equations are solved to calculate hydrodynamic forces developed from the impeller shroud and wear-ring seal. A separation-of-variable solution approach is used for the first-order perturbation equations. By assuming a circular precessional motion, the time dependency in the governing equations is eliminated. A transition-matrix approach (Meirovitch 1985) is used to solve the first-order perturbation equations. The first-order pressure solution is then integrated axially and circumferentially to determine the rotordynamic coefficients. Complete details of the governing equations and solution procedure are given in Ha(1997).

2.3 Determination of rotordynamic coefficients

For small orbital motion of the rotor about a centered position, the forces generated within the impeller shroud and wear-ring seal can be modeled by the set of linearized rotordynamic coefficients.

$$-\begin{Bmatrix}F_x\\F_y\end{Bmatrix}=\begin{bmatrix}K & k\\-k & K\end{bmatrix}\begin{Bmatrix}x\\y\end{Bmatrix}+\begin{bmatrix}C & c\\-c & C\end{bmatrix}\begin{Bmatrix}x'\\y'\end{Bmatrix}+\begin{bmatrix}M & m\\-m & M\end{bmatrix}\begin{Bmatrix}x''\\y''\end{Bmatrix} \tag{9}$$

The theoretical hydrodynamic forces by integrating the first-order pressure solution are given in terms of the radial and tangential force. As shown in Eq. (10), the radial and tangential force components can be stated as a function of f, the ratio of the precession frequency to the rotor speed, by coordinate transformation of Eq. (9).

$$f_r(f)=-K-fc+f^2M \tag{10}$$

$$f_\theta(L)=k-fC-f^2m$$

Briefly, the rotordynamic coefficients are obtained by calculating $f_r(f)$ and $f_\theta(f)$ for a range of f, and then using a least-squares curve fit of Eq. (10). For the range of f, 0.0 to 1.5 is used in present work.

2.4 The rotordynamic coefficients of the impeller shroud and wear-ring seal as a whole

The theoretical analysis for calculating the rotordynamic coefficients of the impeller shroud and wearing seal(Fig. 1) has been carried out based on the previous discussion. The surfaces of the impeller shroud, wear-ring seal and the rotor are smooth and represented by Yamada's(1962) test data. The measured pressure difference between the inlet of the impeller shrouds and the exit of the wear-ring seals are the same for each of the fourteen stages. The input data used in our

Table 1 Input data for the analysis of the impeller shroud and wear-ring seal.

Pressure difference	4.7(bar)
Impeller shroud surface length	40.25(mm)
Radius of impeller shroud inlet	90(mm)
Inlet clearance of impeller shroud	2.67(mm)
Wear-ring seal length	8(mm)
Radius of wear-ring seal	50(mm)
Clearance of wear-ring seal	0.23(mm)
Normalized inlet-tangential velocity	0.25
Inlet loss coefficient(ζ)	0.1
Pressure loss coefficient(C_p)	0.6
Rotor speed	3550(RPM)
Density	1000(kg/m^3)
Absolute viscosity	0.0013(N·s/m^2)
Empirical coefficients (ns, ms) for stator surface	0.079, −0.25
Empirical coefficients (nr, mr) for rotor surface	0.079, −0.25

Table 2 The results of rotordynamic coefficients for the impeller shroud and wear-ring.

K(N/m)	k(N/m)	C(N·s/m)	c(N·s/m)	k/(ωC)
300000	560000	433	-268	3.5

theoretical analysis are listed on Table 1.

The results of the rotordynamic coefficients of one stage are listed on Table 2. As the added mass (M) and cross-coupled mass coefficient(m) are comparatively small, only the rotordynamic coefficients of the direct stiffness(K), cross-coupled stiffness(k), direct damping(C), and cross-coupled damping(c), as well as the whirl frequency ratio, $\frac{k}{\omega C}$, are listed and used for the rotordynamic analysis.

3. Rotordynamic Analysis of Balance Piston and Interstage Seals

The balance piston seal is located next to the last impeller stage and restricts leakage along the rear impeller shroud of the last stage. As the full head rise of the pump is dropped across the balance piston seal, relatively big hydrodynamic forces are generated. The theoretical analysis for calculating rotordynamic coefficients of the balance piston is the same as that of the wear-ring seal part mentioned in the previous section. The surfaces of the balance piston seal and rotor are smooth. The measured pressure difference obtained by the Bourdon pressure gauge is served. Table 3 illustrates the results of the rotordynamic coefficients of the balance piston seal

The interstage seal restricts leakage along the shaft between stages. There are thirteen interstage seals for the fourteen stage centrifugal pump. The surfaces of the interstage seal and rotor are smooth. The pressure difference at each interstage seal can be assumed to be 0. 5 bar because the head rise of one stage is 5.2 bar and it drops as much as 4.7 bar along the impeller shroud and wear-ring seal. The theoretical analysis for calculating rotordynamic coefficients of the interstage seal is the same as that of the balance piston seal except for the surface friction factor model. Flow along the interstage seal is laminar because of the small pressure difference(0.5 bar) and tight clearance. The friction factor model of the turbulent annular seal analysis is modified for laminar seal analysis by (f_s, f_r) = 16/(Reynolds number). Table 4 illustrates the results of the rotordynamic coefficients for one interstage seal.

Table 3 The results of rotordynamic coefficients for the balance piston seal.

K(N/m)	k(N/m)	C(N · s/m)	c(N · s/m)	k/(ωC)
2970000	1840000	164500	2580	0.03

Table 4 The results of rotordynamic coefficients for one interstage seal.

K(N/m)	k(N/m)	C(N · s/m)	c(N · s/m)	k/(ωC)
55500	3560	208	11.4	0.05

4. Finite Element Rotordynamic Modeling of Pump System and Solution Procedure

A rotor-bearing system model of a 750 m-head fourteen-stage centrifugal pump is shown in Fig. 4(a) along with its equivalent finite element model(Fig. 4(b)). Its rating speed is 3550 RPM. The system is composed of the shaft, 14 impellers (D4~D17), two roller bearings, one balance piston(D18:sleeve, D19:seat), half coupling (D1), 14 impeller shroud and wear-ring seals, 13 interstage seals, and other sleeves. The shroud and wear-ring seals and the interstage seals, which are not shown in Fig. 1, are modeled as bearing elements of equivalent stiffness and damping coefficients, and they are assumed to be placed on the associated impeller center locations. Basic modeling data are given in Table 5 and various seal dynamic properties are listed in Tables 2~4.

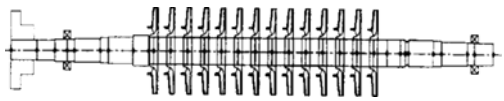

(a) Schematic of a pump rotor-bearing system

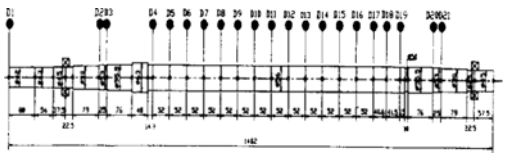

(b) Equivalent finite element model

Fig. 4 A fourteen-stage 750m-head centrifugal pump model.

Table 5 Basic modeling data of pump rotor-bearing system.

	Disk Mass(kg) and Inertia(10^{-3}kg·m^2)	Shaft Material Property
D1	m=6.65, I_t=16.5, I_p=19.1	
D2, D21	m=0.348, I_t=0.212, I_p=0.280	E=2.00×10^{11}N/m^2
D3, D20	m=0.410, I_t=0.852, I_p=0.365	ρ=7830kg/m^3
D4, D17	m=1.93, I_t=3.86, I_p=7.34	Roller Bearing Dynamic Property
D5~D16	m=2.05, I_t=4.02, I_p=7.46	Kxx=KYY
D18	m=0.558, I_t=0.444, I_p=0.541	=5.19×10^{8}N/m
D19	m=1.86, I_t=2.54, I_p=4.96	

The basic finite element building blocks of various component elements, e. g., shafts, disks, and bearings have been derived. They are assembled to give a global system equation under the recognition that when two elements are assembled, the respective generalized displacements at a common node be equal and the respective generalized forces be added. Finally, the resulting system equation are solved by the matrix method.

5. Results of Rotordynamic Analysis and Discussion

5.1 Mode analysis

Dry Mode Analysis: A critical speed map of the pump rotor-bearing system is shown in Fig. 5. Though it has been obtained ignoring any seal effects, it still gives valuable insights into the system. As the bearing stiffness increases over 108^8 N/m, whirl natural frequencies quickly approach asymptotic constant ones. Since the roller bearing stiffness is 5. 19×108 N/m, the first and second whirl natural frequencies are estimated around 2400 and 8600 RPMs. Detailed dry mode analyses give the first and second critical speeds as 2456 (Refer to Fig. 6(a)) and 8930 RPM, which confirm the critical speed map.

Wet Mode Analysis: In wet analyses all seal effects of such as the shroud and wear-ring seals, interstage seals, and balance piston have been considered. For comparison, only the first critical will be considered into as the pump rating speed is 3550 RPM. As shown in Fig. 6(b), the critical

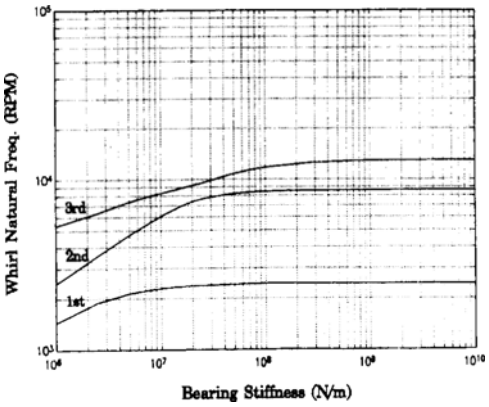

Fig. 5 Critical speed map of the pump rotor-bearing system.

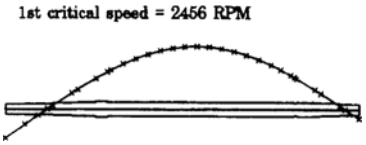

(a) Dry analysis-on seal effects at all

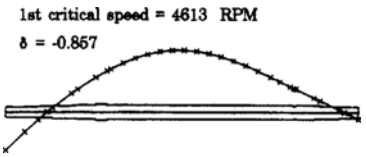

(b) Wet analysis-original shroud and wear-ring seal designs

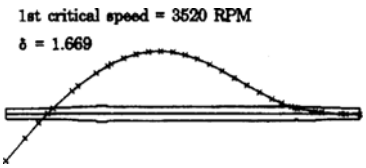

(c) Wet analysis-modified shroud and wear-ring sealdesigns

Fig. 6 Mode shapes and first critical speeds.

speed is 4613 RPM and logarithmic decrement is -0.857. Comparing to the dry mode analysis, the first critical speed is increased considerably because the seals act as additional bearings distributed along the shaft span. However, the logarithmic decrement of -0.857 means that the model system is unstable, and this possibility should be eliminated in the design process. The hydrodynamic forces from fluid-filled gaps

(seals) have been suspected as the source of instability. Particulary, the cross-coupled stiffnesses, which represent circumferential force components in the whirling direction, in seals may represent qualitatively their extent of contribution to system instability. For the stability of each component, the whirl frequency ratio, $\frac{k}{\omega C}$, should be less than 1. The whirl frequency ratios of the impeller shroud and wear-ring seal, the balance piston, and the interstage seal have been calculated at 3550 RPM, and they are summarized in Tables 2~4. While the ratios of the balance piston and the interstage seal are 0.03 and 0.05, the ratio of the impeller shroud and wear-ring seal is 3.477. This may identify the large cross coupled stiffness of the shroud and wear-ring seal as the sourec of the instability.

5.2 Design modification

As the model system is unstable and the impeller shroud and wear-ring seal has been identified as the source of the instability, the efforts have been made to reduce k and increase C in the impeller shroud and wear-ring seal by modifying its geometry. Figure 7 shows the effect of the wear-ring seal clearance on the k and C of the impeller shroud and wear-ring seal. As the wear-ring seal clearance increases from the original clearance, k decreases but C increases slightly. Figure. 8 shows the effect of impeller shroud clearance on the k and C of the impeller shroud and wear-ring seal. As the shroud clearance decreases from the original clearance, k decreases generously but C increases. So in the modified impeller shroud and wear-ring seal, the wear-ring seal and impeller shroud clearances are designed as 0.33 mm and 1.5 mm, respectively. The corresponding modified stiffnesses and dampings are shown in Table 6.

Comparing Table 2 with Table 6, the destabilizing component of k is decreased (43 %) but the stabilizing component of C is much increased (180 %). Thereby, the rotordynamic characteristics are expected to be improved considerably with the modified impeller shroud and wear-ring seal. The modified impeller shroud and wear-ring

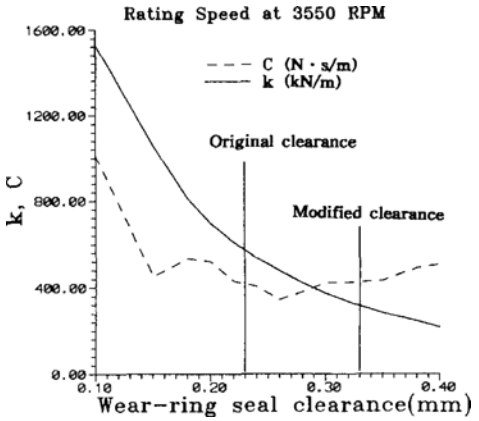

Fig. 7 k and C of the impeller shroud and wear-ring seal versus the wear-ring seal clearance.

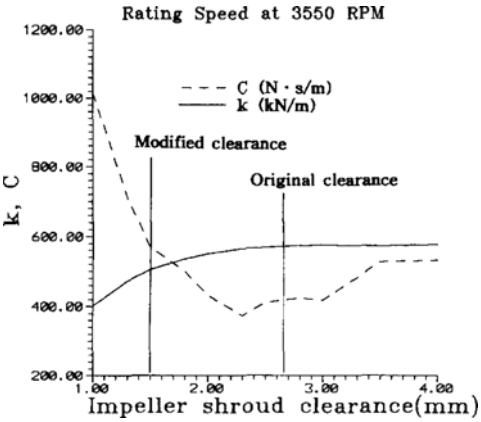

Fig. 8 k and C of the impeller shroud and wear-ring seal versus the impeller shroud clearance.

Table 6 Rotordynamic coefficients for modified design of impeller shroud and wear-ring seal.

K (N/m)	k (N/m)	C (N · s/m)	c (N · s/m)	k/(ωC)
210000	240000	783	-171	0.8

seal yields that the whirl frequency ratio is less than 1. Finally, the critical speed of the modified pump system is 3520 RPM with a logarithmic decrement of 1.669 as shown in Fig. 6(c). Now, the system is predicted as strongly stable. Even though the critical speed is very close to the pump rating speed of 3550 RPM, it should present no concern at all as the system is well damped, i. e., an amplification factor of 1.882.

6. Conclusive Remarks

A modeling methodology of a pump impeller shroud and wear-ring seal as a whole has been developed to give its rotordynamic coefficients, and a detailed rotordynamic analysis has been carried out on a 750 m-head fourteen-stage centrifugal pump system. In the analysis the effects of the hydrodynamic forces such as impeller shroud and wear-ring seals, balance piston, and interstage seals have been taken into account. Since the various seals have acted as additional bearing elements distributed along the shaft span, the first critical speeds of wet mode analyses have been predicted to be higher than that of dry mode analysis as expected.

The wet mode analysis has shown that the system is unstable and large cross coupled stiffness(k) of the impeller shroud and wear-ring seal has been suspected as the source of the instability problem. Therefore, design modifications have been performed to decrease k and increase C by increasing the wear-ring seal clearance and decreasing the impeller shroud clearance simultaneously. For the modified design of the shroud and wear- ring seal, mode analysis has predicted that the system is stable and well damped.

Finally, it is emphasized that to accurately predict the rotordynamic behaviors of multi-stage pump systems and most of all to assure their trouble free designs, the modeling of the impeller shroud and wear-ring seal as a whole needs to be practiced in the design process, and also other seals such as balance pistons and interstage seals need to be included in the modeling.

7. Acknowledgment

This paper was supported by the NON-DIRECTED RESEARCH FUND, Korea Research Foundation, 1996.

References

Atkins, K, E., Tison, J. D., and Wachel, J. C., 1985, "Critical Speed Analysis of an Eight-Stage Centrifugal Pump," *Proceedings of the Second International Pump Users Symposium,* The Turbomachinery Lab., Texas A&M Univ., College Station, Texas, pp. 59~65.

Black, H., and Jenssen, D., 1970. "Dynamic Hybrid Properties of Annular Pressure Seals," *Journal of Mechanical Engineering,* 184, pp. 92~100.

Bowman, D. G., Marsher, W. D., and Reid S. R., 1990, "Pump Rotor Critical Speeds Diagnosis and Solutions," *Proceedings of the Seventh International Pump Users Symposium,* The Turbomachinery Lab., Texas A&M Univ., College Station, Texas, pp. 73~80.

Childs, D., 1983, "Dynamic Analysis of Turbulent Annular Seals Based on Hirs' Lubrication Equation," *Journal of Lubrication Technology,* Vol. 105, pp. 437~444.

Childs, D., 1989, "Fluid-Structure Interaction Forces at Pump-Impeller-Shroud Surfaces for Rotordynamic Calculations," *Journal of Vibrations, Acoustics, Stress, and Reliability in Design,* Vol. 111, pp. 216~225.

Childs, D. W., 1993, *Turbomachinery Rotordynamics Phenomena, Modeling, and Analysis,* John Wiley and Sons, Inc.

Childs, D., and Kim, C. H., 1985, "Analysis and Testing for Rotordynamic Coefficients of Turbulent Annular Seals with Different, Directionally-Homogeneous Surface-Roughness Treatment for Rotor and Stator Elements," *Journal of Tribology,* Vol 107, pp. 296~306.

Frei, A, Guelich, J., Eichhorn, G., and Eberl, J., 1990, "Rotordynamic and Dry Running Behavior of a Full Scale Test Boiler Feed Pump," *Proceedings of the Seventh International Pump Users Symposium,* The Turbomachinery Lab., Texas A&M Univ., College Station, Texas, pp 81~91.

Ha, T. W., 1997, "Rotordynamic Analysis of Impeller Shroud and Wear-ring Seal on Centrifugal Pump," *Proceedings of the KSME 1997 Spring Annual meeting,* Vol. A, pp. 314~320.

Hirs, G., 1973, "A Bulk-Flow Theory for Turbulence in Lubricant Films," *Journal of Lubrication Technology,* pp. 137~146.

Lalanne, M. and Ferraris, G., 1990, *Rotor-*

dynamics Prediction in Engineering, John Wiley and Sons, Inc.

Massey, B., S., *Mechanics of Fluids,* 5th edition, Van Nostrand Reinhold(UK), 1986, pp. 204~205.

Meirovitch, L., 1985, *Introduction to Dynamics and Control,* Wiley, New York.

Nordmann, R., and Massman, H., 1984, "Identification of Dynamic Coefficients of Annular Turbulent Seals," *Rotordynamic Instability Problems in High-Performance Turbomachinery -1984, NASA CP* No. 2338, Proceedings of a Workshop held at Texas A&M University, pp. 295~311.

Ruhl, R. L. and Booker, J. F., 1972, "A Finite Element Model for Distributed Parameter Turborotor Systems," *ASME Trans., Journal of Engineering for Industry,* pp. 126~132.

Wachel, J. C., Atkins, K. E., and Tison, J. D., 1995, "Improved Reliability through the Use of Design Audit," *Proceedings of the Twenty -Fourth Turbomachinery Symposium,* The Turbomachinery Lab., Texas A&M Univ., College Station, Texas, pp. 203~219.

Yamada, Y., 1962, "Resistance of Flow Through an Annulus with an Inner Rotating Cylinder," *Bull JSME, 5(18),* pp. 302~310.

Zorzi, E. S. and Nelson, H. D., 1977, "Finite Element Simulation of Rotor-Bearing Systems with Internal Damping," *ASME Trans., Journal of Engineering for Power,* pp. 71~77.